Contents lists available at ScienceDirect

Engineering in Agriculture, Environment and Food

journal homepage: www.elsevier.com

Field phenotyping using multispectral imaging in pea (*Pisum sativum* L) and chickpea (*Cicer arietinum* L)

Juan J. Quirós [a, b], Rebecca J. McGee [c], George J. Vandemark [c], Thiago Romanelli [b], Sindhuja Sankaran [a, *]

[a] Department of Biological Systems Engineering, Washington State University, Pullman, WA 99164, USA
[b] Department of Biosystems Engineering, Luiz de Queiroz College of Agriculture, ESALQ, University of Sao Paulo, Piracicaba, SP 13418-900 Brazil
[c] USDA-ARS, Grain Legume Genetics and Physiology Research Unit, Pullman, WA 99164-6434, USA

ARTICLE INFO

Keywords:
Field phenomics
NDVI
Breeding
Image analysis

ABSTRACT

Pea (*Pisum sativum* L) and chickpea (*Cicer arietinum* L) are important grain legumes grown in the Palouse region of the Pacific Northwest United States. The USDA-ARS grain legume breeding program in this region focuses on developing pea and chickpea varieties with high yield potential, resistance to biotic and abiotic stresses, and superior agronomic characteristics. In this study, aerial high resolution multispectral imaging was evaluated to phenotype yield potential differences among genotypes in green pea, yellow pea and chickpea. Five experiments (three field pea and two chickpea) with 10–25 varieties grown at two locations (Pullman, Washington; Genesee, Idaho) were assessed. Images were acquired approximately 60, 70 and 90 days after planting (DAP) at 110 above ground level. Normalized difference vegetation index (NDVI), green normalized difference vegetation index, soil adjusted vegetation index (SAVI) and simple ratio (SR) image based features (SUM, MIN, MAX, MEAN) were extracted. In most cases, the MEAN NDVI data was found to be consistently correlated with dry seed yield ($p < 0.05$), with green pea genotypes showing highest correlations with seed yield ($r = 0.64–0.93$ at about 70 DAP, both during "plot-by-plot" and "by genotype" comparisons). The MEAN SAVI and SR values were also strongly correlated with yield at 61–72 DAP in most of the pea experiments. The data collected during flowering and early pod development phenological growth stages was found to be useful in yield estimation. The developed methods can be used for early generation evaluation in breeding programs, where yield cannot be estimated due to limited seed availability.

1. Introduction

Pea (*Pisum sativum* L) and chickpea (*Cicer arietinum* L) are cool season, annual grain legume crops that are produced worldwide for human food and animal feed (McPhee, 2003; Coyne et al., 2011). They are often grown in rotation with small grain cereals to break disease cycles, and their symbiotic relationships with *Rhizobial* bacteria enhances the soil fertility through atmospheric nitrogen fixation. Moreover, these crops are a nutritious source of food, feed and fodder, rich in protein, soluble starch, vitamins, and minerals (Cheng et al., 2015). The pea is also an economically important crop with production in more than 87 countries (McPhee, 2003). The Palouse region, in the Pacific Northwest United States, is one of the leading producers of pea and chickpea in the USA (USDA-NASS 2016). The United States Department of Agriculture- Agricultural Research Service field pea and chickpea breeding program has released several field pea and chickpea cultivars (McPhee and Muehlbauer, 2002, 2004; Muehlbauer et al., 1998, 2004, 2006; McGee et al. 2012, 2013; McGee and McPhee, 2012; Vandemark et al., 2014, 2015) with higher yield potential and stress tolerance.

Phenotyping is a key aspect in plant breeding programs that refers to the evaluation of plant traits (e.g. plant height, pod length) and crop performance (e.g. seed yield, quality) resulting from interaction between the genotype and the environment. In general, field phenotyping is challenging due to tedious in-field measurements requiring significant resources (personnel, time) (Araus and Cairns, 2014). Remote sensing offers a practical alternative for high-throughput crop phenotyping in breeding research plots. Aerial images acquired from satellites and unmanned aerial vehicles (UAVs) have been used for yield estimation in rice (Tennakoon et al., 1992; Swain et al., 2010), sugarcane

* Corresponding author.
Email address: Sindhuja.Sankaran@wsu.edu (S. Sankaran)

https://doi.org/10.1016/j.eaef.2019.06.002
Received 6 December 2018; Received in revised form 9 May 2019; Accepted 10 June 2019
Available online xxx
1881-8366/

(Rao et al., 2002; Murillo and Carbonel, 2012), sunflower (Vega et al., 2015), corn (Shanahan et al., 2001; Fang et al., 2008; Yao et al., 2015), wheat (Serrano et al., 2000; Paiva et al., 2013), cotton (Brandão et al., 2011), and pea (Mkhabela et al., 2011). Most of these studies utilize vegetation indices (VIs), calculated from visible and near infrared (NIR) bands of the electromagnetic spectra, to estimate yield potential. In general, a healthy plant scatters more NIR radiation from cell walls in the mesophyll of the leaves, while visible light is highly absorbed by pigments such as chlorophyll *a* and *b* (Basnyat et al., 2004; Glenn et al., 2008). An increase in chlorophyll content is indicative of higher photosynthetic rates, which can be related to higher yield potential (Sid'ko et al., 2017). VIs such as normalized difference vegetation index (NDVI) capture this differential absorption/reflection in visible and NIR bands, which can be used to infer overall crop health/productivity (Candiago et al., 2015).

In recent years, applications of UAV systems for plant phenotyping have increased. Sensors integrated with UAVs have been used for estimating plant height (Hu et al., 2018), biomass (Quirós et al., 2019; Bendig et al., 2014), and leaf area index (Chen, 2018). UAVs can be integrated with sensors to acquire aerial data at desired spatial and temporal resolution to estimate yield potential (Zhang and Kovacs, 2012). Both, low (multispectral) and high (hyperspectral) spectral resolution sensors can be utilized for this purpose. Although aerial imaging for yield estimation has been explored, there is very limited literature validating this approach in plant breeding programs (Haghighattalab et al., 2016; Shi et al., 2016), given the natural variability between different varieties. The small scale of breeding plots enables the use of multirotor UAVs equipped with multispectral cameras that can acquire useful information for phenotyping applications (Sankaran et al., 2015).

A key aspect for remote sensing-based phenotyping applications is image processing methodologies used to extract features representative of crop traits. Aerial images collected using UAV-based multispectral cameras must be processed accurately in order to extract useable information. For these purposes, it is necessary to create proper image processing protocols for methodologies such as plot segmentation, extraction of VIs, and extraction of summary statistics (minimum, average, maximum and sum of the pixel values within region of interest). This may also include supervised and unsupervised learning pipelines (Bunting et al., 2014; Tagil and Jenness, 2008). Moreover, protocols need to be evaluated and adapted for a specific crop for practical application and rapid extraction of image features representing crop performance traits. Legume crops are different from other crops evaluated in the field conditions (e.g. wheat, corn, rice, etc.), as they are small plants with relatively lower biomass accumulation in comparison to other field crops. The overall goal presented in this work was to validate the technique in legume crops, to assess the applicability of the techniques for phenotyping in legume breeding programs. Therefore, the specific objective of this study was to create a reliable image processing protocol to determine key remote sensing features captured using UAV that could capture differences in yield potential in field pea and chickpea breeding programs. Summary statistic measures of four VIs - NDVI, green NDVI (GNDVI), simple ratio (SR), and soil adjusted vegetation index (SAVI) - were evaluated (Thenkabail and Lyon, 2012).

2. Methods

2.1. Field plots

Data were collected from two field locations: Pullman, Washington (46°42′0.12″ N, −117° 8′18.26″ W) and Genesee, Idaho (46°36′20.43″ N, −116°58′13.86″ W). The Pullman and Genesee field sites with breeding plots are shown in Figs. 1 and 2. The pea/chickpea plots were planted in Genesee and Pullman on 21 April 2015 and 26 April 2015, respectively. A seed treatment was applied to all seeds prior to planting that contained fludioxonil (0.56 g kg^{-1}, Syngenta, Greensboro, North Carolina, USA), mefenoxam (0.38 g kg^{-1}, Syngenta, Greensboro, North Carolina, USA), and thiabendazole (1.87 g kg^{-1}, Syngenta, Greensboro, North Carolina, USA), thiamethoxam (0.66 ml kg^{-1}, Syngenta, Greensboro, North Carolina, USA), and molybdenum (0.35 g kg^{-1}). About 0.5 g Mesorhizobium ciceri inoculant (1×10^8 CFU g^{-1}; Novozyme, Cambridge, Massachusetts, USA) was added to each chickpea seed packet 1 day prior to planting. Peas and chickpeas were planted at a density of 86 seeds m^{-2} and 43 seeds m^{-2}, respectively, in about 1.5 × 5.0 m plots. Weeds were controlled by a single post-plant/pre-emergence application of metribuzin (0.42 kg ha^{-1}, Bayer Crop Science, Raleigh, North Carolina, USA) and linuron (1.34 kg ha^{-1}, NovaSource, Phoenix, Arizona, USA).

A randomized complete block design with three replications was used for all field location experiments (Fig. 2). The three pea exper-

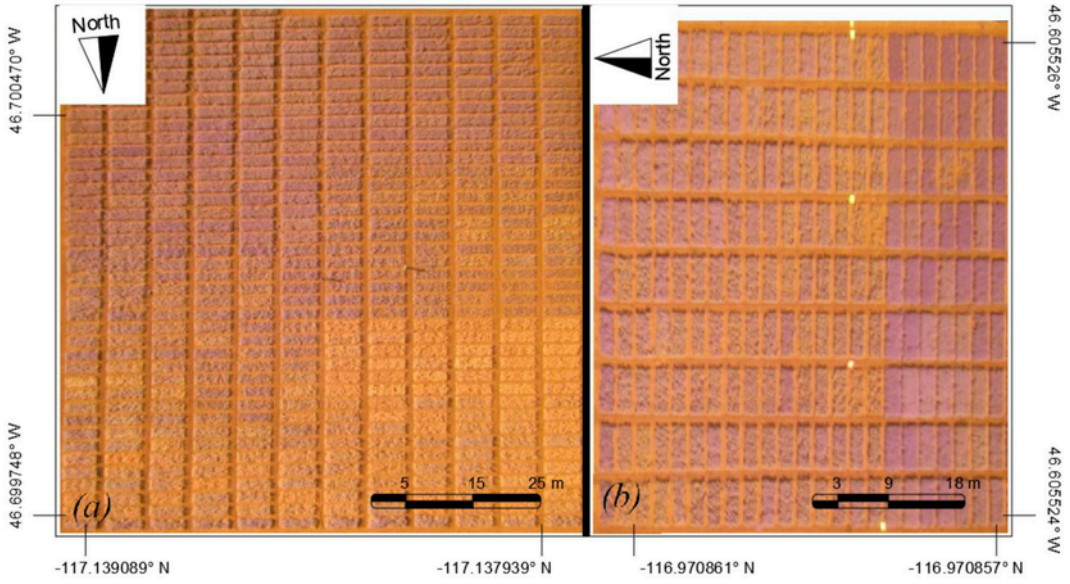

Fig. 1. False colour aerial images (R, G, NIR) of plots at 61 days after planting in Pullman (a), and 68 days after planting in Genesee (b). (For interpretation of the references to colour in this figure legend, the reader is referred to the Web version of this article.)

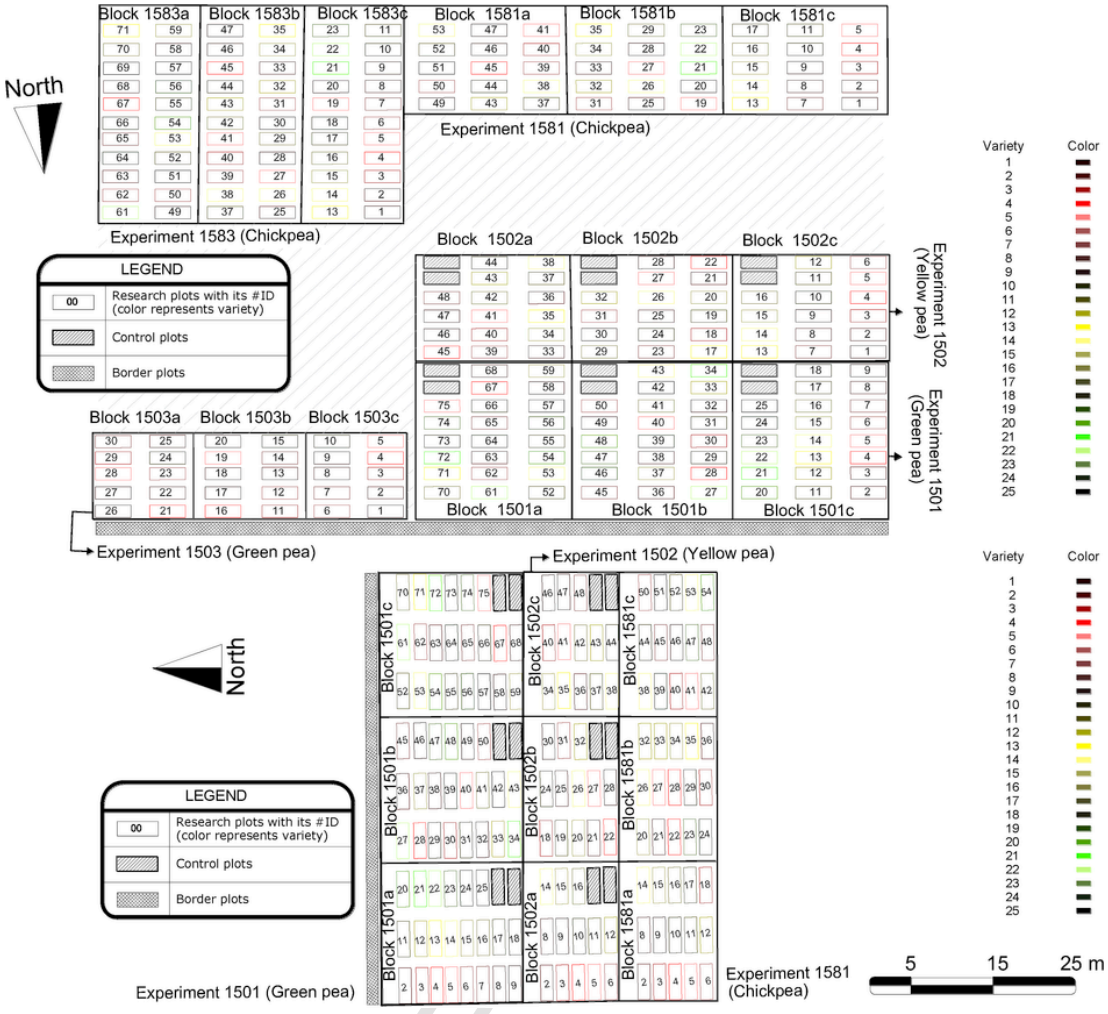

Fig. 2. Distribution of experiments, blocks, and plots in Pullman (a) and Genesee (b) field sites showing the randomized complete block design with three replicate plots. Genotype/variety are differentiated based on the colour scale. Note: The varieties between experiments are different. For example, genotype/variety 1 in 1501 does not correspond to the same genotype/variety in experiment 1502 or 1581. (For interpretation of the references to colour in this figure legend, the reader is referred to the Web version of this article.)

iments at the Pullman field site were labelled as 1501, 1502, and 1503 and contained 75, 48 and 30 plots, respectively. The number of genotypes and breeding lines (genotypes) planted in 1501 was 25 (green pea), experiment 1502 was 16 (yellow pea), and experiment 1503 was 10 (green pea). Chickpea experiments in Pullman were labelled as 1581 and 1583 with 54 and 72 plots (18 and 24 genotypes), respectively. At the Genesee field site, pea experiments 1501 and 1502, and chickpea experiment 1581 were planted with the same experimental design, number of plots, and genotypes as those described for the Pullman field site. Each block had the same number of plots. The field site was maintained based on standard procedures used by the grower in the Palouse region. Plots were harvested using a Zurn® 150 plot combine and seed was further cleaned mechanically with an air blower. Seed yield was computed per plot and converted into kg ha^{-1}.

2.2. Data collection

The UAV-multirotor OktoXL 6S12 (HiSystems GmbH, Moormerland, Germany) was used for imaging the field plots. The platform was powered by a 6500 mAh Lithium-ion polymer battery, and was capable of manual and automated control. For data acquisition in the present study, the UAV was manually controlled with a 4-km radio transmitter (MX20 Hott, Graupner, Stuttgart, Germany). The flight time was approximately 10 min. The sensor used was a 3-band modified multispectral camera (Canon Powershot ELPH 340 HS, LDC LLC, Carlstadt, New Jersey, USA), which captures the relative reflectance as digital numbers (DN) in the red (R), green (G), and near infrared (NIR, 800–900 nm) regions of the electromagnetic spectrum. The camera was placed on a gimbal that could adjust the position of the camera during the flight. The firmware was set to acquire images at 0.2 Hz. The 8-bit, 16-megapixel images were stored on the camera's memory card. Flight height was set at 110 m above ground level (AGL) (GSD = 3.5 cm) based on Sankaran et al. (2018), where the GNDVI data acquired at 50 m and 120 m AGL imagery were similar, and were highly correlated ($r = 0.95$; $P < 0.0001$). At this altitude, the entire field plots were captured, which eliminated the need for image stitching as well.

In 2015, at the Pullman field site, aerial images were acquired at 61, 72, and 89 days after planting (DAP). At 89 DAP, the pea trials 1502 were harvested due to early senescence. At the Genesee field site, images were acquired at 68 DAP and 94 DAP. At both locations, at the 61 DAP imaging, the pea plants were at growth stages between 3 and 4; at 68–72 DAP, the pea plants were at growth stages between 5 and 6; and at 89–94 DAP, the pea plants were at growth stages between 6 and 7 (Kalu and Fick, 1981). The growth stages 3–7 represent early budding, late budding, early flowering, later flowering, and early seed pod development morphological stages, respectively, as described by Kalu and Fick (1981). At both locations, at 61 DAP, chickpeas were at approximate growth stage R2 (full bloom); at 72 DAP between growth

stages R3 (early pod visible) and R4 (when pod has reached full size and is largely flat); and at 89 DAP chickpeas were between R6 (full seed) and R7 (leaves start to yellow and 50% of 153 pods are yellow) (Saxena and Hawtin, 1981). A 25 × 25 cm white reference panel (Spectralon Reflectance Target, CSTM-SRT-99-100, Spectra Vista Cooperation, New York, USA) was used for radiometric correction during data collection. Table 1 lists the image features and statistic measures extracted from data for each location and data collection period.

2.3. Image processing

ArcGIS® (10.2, ESRI, Redlands, California, USA) software was used for all raster and vector data processing as detailed in following sections. In ArcGIS, the vector processing in ArcGIS represents position coordinates, while raster processing refers to grids cells made up of pixels. Summary statistic measures were extracted from each plot using variable digital numbers of the image pixels extracted from the VIs (NDVI, GNDVI, SR, and SAVI) in this study. The measures extracted were mean (MEAN), maximum (MAX), minimum (MIN) and summation (SUM). The MEAN refers to the average of the pixel values found within each plot polygon; the MAX and MIN represent the highest and lowest pixel values within each polygon that delimits a plot; and SUM refers to the sum of all pixel values within a polygon or plot. Fig. 3 summarizes the image processing steps.

2.3.1. Radiometric correction (raster processing)

Post-image acquisition, radiometric correction was performed (Fig. 3a). Prior to the UAV flight mission, the reference panel was imaged at less than 5 m AGL. From this image, a polygon enclosing the reference panel (99% reflectance in visible-near infrared spectra) was manually generated and maximum 8-bit grey level for each band was set to 255. The DN or pixel value of each pixel of individual band within the image was corrected accordingly. After radiometric correction, the corrected DN represents reflectance data as the image DN data were corrected for incident solar radiation.

2.3.2. VI calculation (raster processing)

In the second step of raster data processing (each time point and location image), NDVI (Equation (1)), GNDVI (Equation (2)), SR (Equation (3)) and SAVI (Equation (4)) images were generated using map algebra (Shirabe, 2011) with red, green and NIR bands from the radiometrically corrected images (Fig. 3b).

Table 1
List of image features and statistic measures extracted from each experiments at each location and data collection period.

Location	Data collection (DAP)	Features extracted	Statistic measures	Experiments
Pullman	61	NDVI	MEAN-SUM-MAX-MIN	1501
		GNDVI	MEAN-SUM-MAX-MIN	1502
		SR	MEAN-SUM-MAX-MIN	1503
		SAVI	MEAN-SUM-MAX-MIN	1581 1583
	72	NDVI	MEAN-SUM-MAX-MIN	1501
		GNDVI	MEAN-SUM-MAX-MIN	1502
		SR	MEAN-SUM-MAX-MIN	1503
		SAVI	MEAN-SUM-MAX-MIN	1581 1583
	89	NDVI	MEAN-SUM-MAX-MIN	1501
		GNDVI	MEAN-SUM-MAX-MIN	1502*
		SR	MEAN-SUM-MAX-MIN	1503
		SAVI	MEAN-SUM-MAX-MIN	1581 1583
Genesee	68	NDVI	MEAN-SUM-MAX-MIN	1501
		GNDVI	MEAN-SUM-MAX-MIN	1502
		SR	MEAN-SUM-MAX-MIN	1581
		SAVI	MEAN-SUM-MAX-MIN	
	94	NDVI	MEAN-SUM-MAX-MIN	1501
		GNDVI	MEAN-SUM-MAX-MIN	1502
		SR	MEAN-SUM-MAX-MIN	1581
		SAVI	MEAN-SUM-MAX-MIN	

*No data available at this data point. Plots were harvested due to early senescence.

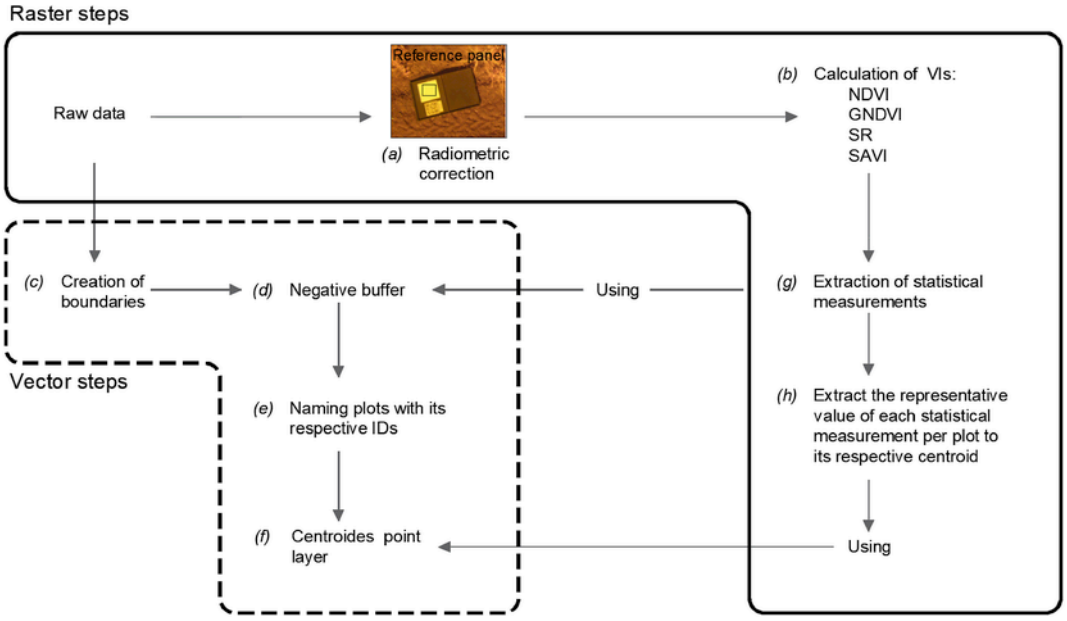

Fig. 3. Raster and vector data processing steps. Solid line encloses steps in raster processing, and dashed line encloses steps in vector processing. The centroid point layer records the statistical measurements (MEAN, SUM, MIN, MAX) for individual plots (5.55 sq. m), excluding the buffer zone.

$$NDVI = \frac{(R_{NIR} - R_R)}{(R_{NIR} + R_R)} \quad (1)$$

$$GNDVI = \frac{(R_{NIR} - R_G)}{(R_{NIR} \mp R_G)} \quad (2)$$

$$SR = \frac{(R_{NIR})}{(R_R)} \quad (3)$$

$$SAVI = \frac{1.5 \times (R_{NIR} - R_R)}{(R_{NIR} + R_R + 0.5)} \quad (4)$$

where R refers to corrected DN (representing reflectance) at NIR, R and G spectral bands.

2.3.3. Plot digitization (vector processing)

The goal for vector processing was to generate a layer of data, where each plot is represented by a data point to allow extraction of statistical measures. The first step of plot digitization was to create the polygons enclosing the entire area of each plot (Fig. 3c). Following this, a negative buffer was created using the "buffer" command in ArcGIS (Fig. 3d), that comprised of the creation of parallel boundary lines towards the interior of the plot (as recommended in Bareth et al., 2015). This was performed to eliminate border effects and avoid interference of border region crop anomalies on the extracted features. The distance between the original plot border and the one created with the negative buffer was 15 cm. With this border area elimination, the 74% of plot cover was retained. For correct plot identification, each polygon was labelled with a specific ID based on the location, time of imaging, and experiment (Fig. 3e and f). All extracted statistical measures (features) per plot and the seed yield data were associated based on this unique plot ID.

2.3.4. Feature extraction

Summary statistical measures (MEAN, MAX, MIN and SUM) representing average, maximum, minimum, and sum of corrected DN data for each plot were extracted from the NDVI, GNDVI, SR and SAVI images (Fig. 3g). These measures were summarized based on the plot ID (Fig. 3h).

2.4. Statistical analysis

The resulting point layer attributes table with the summary of image features statistical measures was exported to a text file. SAS version 9.3 (SAS Institute, Raleigh, North Carolina, USA) was used to calculate the Pearson's correlation coefficients (r) between the four statistical measurements (SUM, MIN, MAX, MEAN) of all VIs (NDVI, GNDVI, SR and SAVI) and seed yield based on 'plot-to-plot' and average 'by genotype' data (from three replicate plots). The results are organized by experiment, time of imaging, location, and vegetation index for the two locations and the two types of analysis (plot-to-plot and by genotype).

3. Results and discussion

3.1. Correlations between NDVI and GNDVI statistical measures with seed yield

Table 2 summarizes the correlation between the statistical measures (SUM, MIN, MAX, MEAN) derived from NDVI/GNDVI images and seed yield based on different imaging periods (DAP), experiments (1501, 1502, 1503, 1581, 1583), type of comparison ("plot-by-plot", "by genotype"), and location (Pullman, Genesee). At Pullman, both chickpeas and peas were negatively affected by residual herbicide, resulting in poor performance of chickpeas, in experiments 1581 and 1583, and early senescence of peas, in experiments 1502 and 1503. Nevertheless, as our goal was to identify the image features representing seed yield potential different between genotypes and identify the right time point for multispectral imaging, the acquired data was considered valid and useful.

During "plot-by-plot" data analysis, the MEAN NDVI was significantly correlated with seed yield in chickpea ($r = 0.33$–0.71) at about 70 DAP. In pea, the correlation coefficients between MEAN NDVI/GNDVI were significant ("plot-by-plot" analysis) at about both 60 and 70 DAP ($r = 0.31$–0.93, Fig. 4). Among different experiments, exper-

Table 2
Correlations coefficient (*r*) between pea (experiments 1501, 1502 and 1503) and chickpea (experiments 1581 and 1583) with seed yield and image features for each experiment with respect to dispersion statistics, DAP, vegetation indices NDVI and GNDVI, and location.

Dispersion statistics	Feature	Pullman						Genesee			
		DAP	1501	1502	1503	1581	1583	DAP	1501	1502	1581
Plot-by-plot											
SUM	NDVI	61	0.61	0.76	0.79	0.18*	0.05*		–	–	–
	GNDVI		0.28	0.65	0.57	−0.00*	0.12*		–	–	–
	NDVI	72	0.74	0.34	0.93	0.42	0.49	68	0.74	0.60	−0.43
	GNDVI		0.70	0.27*	0.71	0.04*	0.42		0.35	0.60	0.58
	NDVI	89	−0.33	–	0.04*	−0.17*	0.52	94	0.75	0.11*	−0.29*
	GNDVI		−0.15*	–	0.49*	−0.43	0.39		−0.05*	−0.33	−0.71
MIN	NDVI	61	0.55	0.57	0.51	0.21*	−0.01*		–	–	–
	GNDVI		0.33	0.65	0.54	0.01*	0.00*		–	–	–
	NDVI	72	0.60	0.46	0.41	0.42	0.21*	68	0.51	0.50	0.68
	GNDVI		0.51	0.42	0.18	0.44	0.14*		0.46	0.58	0.66
	NDVI	89	0.14*	–	0.37*	−0.18*	0.54	94	0.46	0.02*	−0.54
	GNDVI		−0.13*	–	0.14*	−0.06*	0.50		0.64	−0.09*	−0.57
MAX	NDVI	61	0.06*	0.35	0.47	0.06*	−0.22*		–	–	–
	GNDVI		−0.04*	0.12*	0.24*	0.27*	−0.12*		–	–	–
	NDVI	72	0.62	0.45	0.86	0.30*	0.30*	68	0.73	0.49	0.63
	GNDVI		0.45	0.38	0.65	−0.02*	0.22*		0.59	0.46	0.43
	NDVI	89	−0.29	–	−0.12*	−0.44	0.48	94	0.29	−0.10*	−0.68
	GNDVI		−0.28	–	−0.27*	−0.44	0.40		0.29	−0.18*	−0.69
MEAN	NDVI	61	0.62	0.76	0.79	0.18*	0.04*		–	–	–
	GNDVI		0.36	0.65	0.57	0.04*	0.32*		–	–	–
	NDVI	72	0.84	0.45	0.93	0.41	0.33	68	0.74	0.60	0.71
	GNDVI		0.56	0.31	0.91	0.53	0.04*		0.72	0.61	0.58
	NDVI	89	−0.24	–	0.14*	−0.20*	0.53	94	0.75	0.02*	−0.70
	GNDVI		−0.41	–	−0.22*	−0.21*	0.45		0.73	−0.33*	−0.75
By genotype											
SUM	NDVI	61	0.84	0.76	0.86	0.12*	0.03*		–	–	–
	GNDVI		0.73	0.60	0.70	0.06*	0.13*		–	–	–
	NDVI	72	0.81	0.63	0.81	0.21*	0.22*	68	0.64	0.48*	0.49
	GNDVI		0.71	0.51	0.58	−0.20*	0.29*		0.45	0.46*	0.67
	NDVI	89	0.69	–	−0.13*	−0.08*	0.78	94	0.65	0.20*	0.06*
	GNDVI		0.05*	–	−0.24*	−0.20*	0.30*		0.34*	−0.48*	0.38*
MIN	NDVI	61	0.73	0.50	0.75	−0.03*	−0.01*		–	–	–
	GNDVI		0.59	0.43*	0.54*	0.44*	0.01*		–	–	–
	NDVI	72	0.61	0.55	0.45	0.33*	0.02*	68	0.50	0.59	0.49
	GNDVI		0.68	0.48*	0.24*	0.33*	−0.06*		0.55	0.55	0.74
	NDVI	89	0.75	–	0.15*	0.01*	0.81	94	0.50	−0.12*	−0.01*
	GNDVI		0.49	–	0.20*	0.14*	0.57		0.54	−0.20*	−0.08*
MAX	NDVI	61	0.34*	0.27*	−0.01*	0.32*	−0.22*		–	–	–
	GNDVI		0.14*	−0.06*	−0.30*	0.10*	−0.12*		–	–	–
	NDVI	72	0.75	0.57	0.88	0.10*	0.28*	68	0.58	0.41*	0.51
	GNDVI		0.63	0.29*	0.67	0.23*	0.22*		0.50	0.32*	0.52
	NDVI	89	0.64	–	−0.40*	−0.13*	0.73	94	0.32	−0.36*	−0.53
	GNDVI		0.27*	–	−0.13*	−0.31*	0.48		0.24*	−0.45*	−0.55
MEAN	NDVI	61	0.84	0.76	0.84	0.13*	0.01*		–	–	–
	GNDVI		0.71	0.35*	0.27*	0.10*	0.03*		–	–	–
	NDVI	72	0.80	0.69	0.81	0.31*	0.10*	68	0.64	0.48*	0.70
	GNDVI		0.70	0.49*	0.61	0.20*	0.17*		0.66	0.46*	0.67
	NDVI	89	0.71	–	−0.21*	0.09*	0.78	94	0.65	−0.29*	−0.45*
	GNDVI		0.39*	–	−0.30*	−0.18*	0.57		0.50	−0.48*	−0.36*

*$p > 0.05$ (not significant at 5% confidence interval).

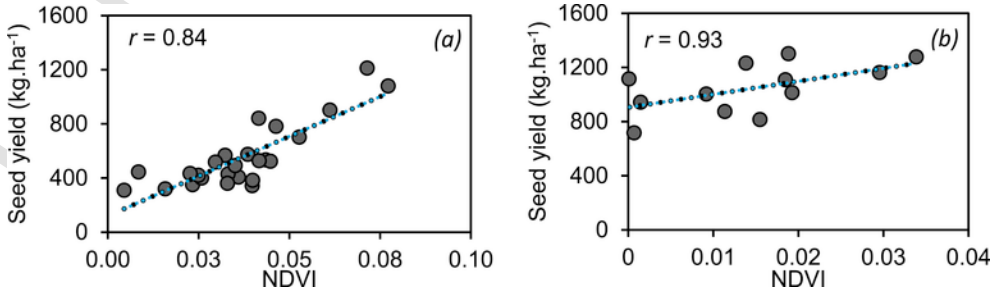

Fig. 4. Correlation between seed yield and average MEAN-NDVI ("plot-by-plot" analysis) at 72 DAP in Pullman field site, experiments (a) 1501 and (b) 1503.

iment 1503 showed the highest correlations between NDVI-based SUM, MAX, and MEAN data with seed yield, using both "plot-by-plot" and "by genotype" data comparisons, especially when the features were derived from data collected at 72 DAP ($r = 0.81–0.93$). In regard to correlation analysis "by genotype", the green pea experiments (1501) from Pullman performed better than Genesee (1501) using MEAN NDVI data at about 70 DAP. Remote sensing data acquired at this time point was useful in identifying high yielding genotypes, as these genotypes were found to be associated with higher vegetation index values. The MEAN NDVI data (at about 70 DAP) from green pea experiments were correlated with seed yield ("by genotype") in both Pullman and Genesee; while the data from yellow pea was only correlated with seed yield in Pullman. This could be attributed to differences in pea type. The yellow pea plants have a pale yellow-green foliage compared to green peas, which could have resulted in less variability in the NDVI data. In most comparisons, the correlation between MEAN NDVI (both "plot-by-plot" and "by genotype" analysis) data and seed yield was consistent and significant when data was acquired at 68 DAP. Similar strong correlations have been found in other crops such as sunflower (Vega et al., 2015), where NDVI data was found to be highly correlated to grain yield ($r = 0.69–0.77$) with images acquired during sunflower's R1 growth stage (floral button formation beginning). In both our study and Vega et al. (2015), strong correlations of NDVI and yield were found when images were acquired during reproductive growth.

Among the different statistical parameters (MIN, MAX, SUM, MEAN), the SUM and MEAN features (followed by MIN) showed consistent and comparable correlation with seed yield potential. Comparing the MEAN-NDVI and -GNDVI data with seed yield, the MEAN-NDVI resulted in higher correlation coefficients than MEAN-GNDVI. To summarize, at both locations, MEAN NDVI data extracted from images acquired at during flowering and early pod development was found to be strongly correlated with seed yield data. The strong correlation at mid-season in spring wheat and field pea has been also reported in Basnyat et al. (2004), where correlation between satellite-image based NDVI data with grain yield was studied. According to Munier-Jolain et al. (2010), at the flowering/early pod development phenological growth stages, the plants maximise their radiation use efficiencies, in order to increase their photosynthetic activity to create assimilates to supply the reproductive organs. In this study, strong correlations between NDVI data and seed yield at flowering/early pod development stages confirm that this stage is critical in predicting the overall crop performances.

3.2. Correlations between SAVI and SR statistical measures with seed yield

NDVI and GNDVI sensitivity can be limited by saturation to high biomass content. This saturation can occur a few weeks before other indexes such as SAVI (Qi et al., 1994). NDVI is a non-linear transformation of the SR. This indicates that variation in plant biomass can be captured using NDVI and GNDVI under low to medium biomass conditions. In contrast, SR has better performance in capturing spatial and spectral variations in the canopy, even under high biomass conditions (Huete et al., 1997). Huete et al. (1997) reported that SR and SAVI were marginally affected by small increments in biomass, and the effect of biomass was much lower in these features than NDVI and GNDVI. Although, legume crops have lower biomass than some other field crops (e.g. wheat), SR and SAVI-based features were also evaluated in this study. In Table 3, statistical measurements (SUM, MIN, MAX, MEAN) extracted from SR and SAVI images were calculated for both pea (1501, 1502, 1503) and chickpea (1581, 1583) experiments and correlated with the seed yield. There was a high correlation between MEAN SR and SAVI with seed yield in green pea experiments from Pullman (61 and 72 DAP), and in green pea and chickpea experiments from Genesee (68 DAP). As with MEAN NDVI data, higher correlations between seed yield and image-based data was found in experiments 1501 and 1503 (green pea genotypes) at 72 DAP in Pullman (Fig. 5) than experiment 1502 (yellow pea genotypes). In addition to MEAN SR/SAVI data, high r values were also found with MAX SR/SAVI data for both "plot-by-plot" and "by genotype"; especially for experiments 1501 and 1503 (green pea) at both locations, with data acquired at about 70 DAP. Chickpea experiment 1581 had stronger relation between seed yield with MEAN and MAX SR/SAVI data at Genesee only (68 DAP), during both "plot-by-plot" and "by genotype" analysis.

Vegetation indices, such as NDVI and GNDVI data, get saturated at growth stages with high vegetative growth, when sensitivity to changes in biomass is lost (Zając et al., 2012; Gu et al., 2013). The MIN/MAX NDVI and GNDVI data could have been contributed from non-canopy objects in the region of interest (e.g. soil, weeds, anomalies). However, the MAX feature of SAVI are not affected in high biomass content. SAVI/SR data are also affected less by saturation (Xiao et al., 2002; Wang et al., 2003). Stress conditions can also induce early senescence in crops (Munier-Jolain et al., 2010). In summary, seed yield of green peas (1501 and 1503) in Pullman, correlated well with the MEAN SR/SAVI "by genotype" and "plot-by-plot" data from images acquired at 72 DAP, and yellow peas at 61 DAP. Chickpea experiment 1581 showed good correlation between seed yield and MEAN SR/SAVI data values at about 70 DAP in Genesee (both "plot-by-plot" and "by genotype"). The environmental conditions can directly impact the phenotype expression (Dhond et al., 2013). In addition, the influence of the residual herbicide could have affected the performance of certain chickpea varieties.

In general, imaging and extracting MEAN data during flowering/early pod development resulted in good estimates of yield potential. In other crops, such as wheat, strong linear regression between NDVI estimates and seed yield ($R^2 = 0.82$; three cultivars, four environments) were reported during UAV-based imaging at flowering stage (Duan et al., 2017). Zhou et al. (2017) reported that the best relationship between grain yield and NDVI data ($r = 0.76$) in rice at the beginning of the reproductive phase (booting and heading stages). Similar results were also found in soybean (Yu et al., 2016), where geometric features extracted using Random Forest algorithm was found to be correlated with yield at advanced reproductive stages (R4-R5 growth stages, $r = 0.82$, $p < 0.01$). Fig. 6 shows the performance of genotypes based on its yield potential and vegetation index data that are highly correlated with their performance (e.g., MEAN SR at 72 DAP). It can be observed that the plots with high VI values are indicative of high yield potential.

The application of modified digital camera could influence the results, especially since the NIR band captured broad wavelength region (800–900 nm). Sensors with independent NIR channel and narrow wavelength range are more reliable in accurately estimating crop parameters, although commercial modified cameras show high promise in crop monitoring applications (Lebourgeois et al., 2008). Factors such as season, time of the day, and developmental stage can also influence data interpretation (Pratap et al., 2019), which needs to be considered during data collection.

4. Conclusions

In this study, UAV-based multispectral images acquired at 60–90 DAP from five experiments (two green pea, one yellow pea, and two chickpea) with 10–25 genotypes, were processed to phenotype differences in seed yield potential. The image features extracted were NDVI, GNDVI, SAVI and SR-based SUM, MIN, MAX, MEAN data were correlated with seed yield. The major findings are as follows:

Table 3
Correlations coefficient (*r*) between pea (experiments 1501, 1502 and 1503) and chickpea (experiments 1581 and 1583) with seed yield and image features for each experiment with respect to dispersion statistics, DAP, vegetation indices SR and SAVI, and location.

Dispersion statistics	Feature	Pullman						Genesee			
		DAP	1501	1502	1503	1581	1583	DAP	1501	1502	1581
Plot-by-plot											
SUM	SR	61	0.37	0.76	0.79	0.10*	0.23*		–	–	–
	SAVI		0.61	0.86	0.79	0.15*	0.23*		–	–	–
	SR	72	0.70	0.08*	0.61	−0.07*	0.52	68	0.74	0.60	0.28
	SAVI		0.74	−0.14*	0.92	0.42*	0.49		0.74	0.60	0.79
	SR	89	0.20*	–	−0.27*	−0.47	0.59	94	0.75	0.05*	−0.70
	SAVI		−0.33	–	0.04*	−0.17*	0.54		0.75	0.05*	0.00*
MIN	SR	61	0.56	0.58	0.51	0.06*	−0.02*		–	–	–
	SAVI		0.55	0.57	0.51	0.06*	−0.01*		–	–	–
	SR	72	0.56	0.43	0.41	0.33*	0.21*	68	0.49	0.50	0.69
	SAVI		0.60	0.43	0.41	0.32*	0.21*		0.51	0.50	0.68
	SR	89	0.14*	–	0.37	−0.17*	0.53	94	0.46	0.02*	−0.55
	SAVI		0.14*	–	0.37	−0.18*	0.54		0.46	0.02*	−0.54
MAX	SR	61	0.21*	0.57	0.71	0.16*	−0.19*		–	–	–
	SAVI		0.06*	0.35	0.46	0.21*	−0.22*		–	–	–
	SR	72	0.63	0.19*	0.86	0.26*	0.30	68	0.73	0.49	0.63
	SAVI		0.62	0.20*	0.86	0.25*	0.30		0.73	0.50	0.63
	SR	89	−0.33*	–	0.45	0.06*	0.52	94	0.29	−0.16*	−0.02*
	SAVI		−0.29*	–	−0.12*	−0.43*	0.48		0.29	−0.10*	−0.68
MEAN	SR	61	0.21*	0.57	0.71	0.18*	0.06*		–	–	–
	SAVI		0.62	0.76	0.79	0.18*	0.04*		–	–	–
	SR	72	0.75	0.45	0.92	0.48	0.33	68	0.74	0.60	0.72
	SAVI		0.74	0.44	0.92	0.48	0.33		0.74	0.60	0.71
	SR	89	−0.26	–	0.13*	−0.08*	0.53	94	0.75	0.02*	−0.69
	SAVI		−0.24	–	0.14*	−0.09*	0.53		0.75	0.02*	−0.70
By genotype											
SUM	SR	61	0.81	0.77	0.81	0.04*	0.23*	–	–	–	–
	SAVI		0.84	0.76	0.86	0.12*	0.03*	–	–	–	–
	SR	72	0.75	0.04*	0.70	−0.24*	0.27*	68	0.64	0.48*	0.47
	SAVI		0.81	−0.16*	0.81	0.21*	0.22*		0.64	0.48*	0.75
	SR	89	0.41	–	−0.10*	0.23*	0.41	94	0.65	−0.20*	−0.46*
	SAVI		0.70	–	−0.13*	0.09*	0.78		0.65	−0.20*	0.14*
MIN	SR	61	0.74	0.51	0.76	−0.02*	−0.02*		–	–	–
	SAVI		0.73	0.50	0.75	−0.03*	−0.01*		–	–	–
	SR	72	0.61	0.50	0.45*	0.33*	0.03*	68	0.49	0.59	0.69
	SAVI		0.61	0.49	0.46*	0.33*	0.02*		0.51	0.59	0.68
	SR	89	0.23*	–	0.16*	−0.38*	0.40*	94	0.50	−0.13*	−0.01*
	SAVI		0.75	–	0.15*	0.01*	0.81		0.46	−0.12*	−0.01*
MAX	SR	61	0.44	0.71	0.83	0.08*	−0.19*	–	–	–	–
	SAVI		0.34*	0.27*	−0.01*	0.32*	−0.22*	–	–	–	–
	SR	72	0.76	0.19*	0.87	0.12*	0.28*	68	0.58	0.41*	0.49
	SAVI		0.75	0.21*	0.88	0.11*	0.28*		0.58	0.41*	0.49
	SR	89	0.45	–	−0.82	0.51	0.59	94	0.32*	−0.36*	−0.43*
	SAVI		0.61	–	−0.40*	−0.13*	0.73		0.02*	−0.36*	−0.53
MEAN	SR	61	0.81	0.77	0.83	0.08*	−0.20*	–	–	–	–
	SAVI		0.84	0.76	0.84	0.12*	0.01*	–	–	–	–
	SR	72	0.81	0.10*	0.80	0.31*	0.11*	68	0.64	0.48*	0.69
	SAVI		0.80	0.69	0.81	0.31*	0.10*		0.64	0.48*	0.70
	SR	89	0.64	–	−0.23*	−0.02*	0.71	94	0.65	0.30*	0.01*
	SAVI		0.70	–	−0.21*	−0.09*	0.78		0.65	0.29*	0.45*

*$p > 0.05$ (not significant at 5% confidence interval).

- The MEAN NDVI data was found to be consistently strongly correlated with pea and chickpea seed yield, especially when derived from images collected during flowering/early pod development.
- The MEAN and MAX SR/SAVI also showed strong correlation when the data was derived from early budding and flowering growth stages in pea plants.
- The correlation results between image features and yield potential analysed "by genotype" was comparable to when analysed "by plot", especially in green pea varieties.
- Between multiple species, the correlation between image features and seed yield potential in green pea genotypes was consistently higher than those in yellow pea and chickpea. The reason for this observation could be because of pale green canopy colour and lower canopy vigour (biomass) in yellow pea and chickpea genotypes, respectively.

In summary, extracting MEAN NDVI from plots at early budding and flowering growth stages can capture differences in seed yield potential between genotypes. Such data can be acquired during early generation stages within a breeding program, where genotype evaluations cannot be performed in plot level due to limited availability of seeds.

Acknowledgements

The authors would like to sincerely thank Dr. Lav R. Khot, Center for Precision and Automated Agricultural Systems, Washington State University for remote sensing data collection. This activity was funded,

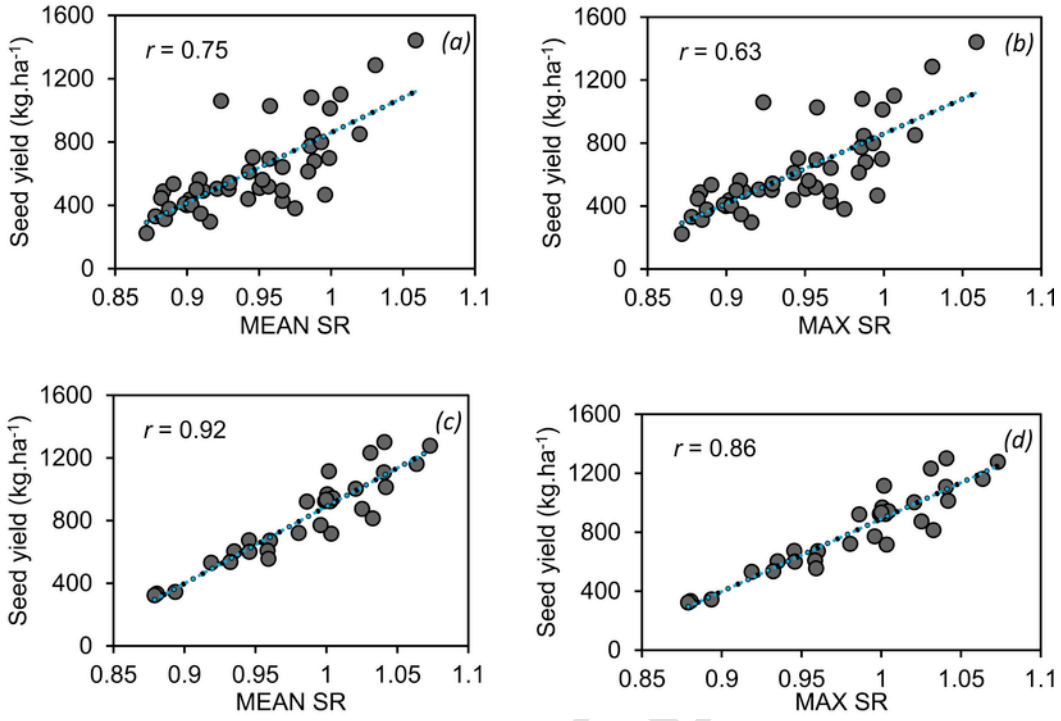

Fig. 5. Correlation of seed yield with MEAN SR and MAX SR in experiments (a and b) 1501 and (c and d) 1503, extracted from individual images at 72 DAP in Pullman field site using "plot-by-plot" data.

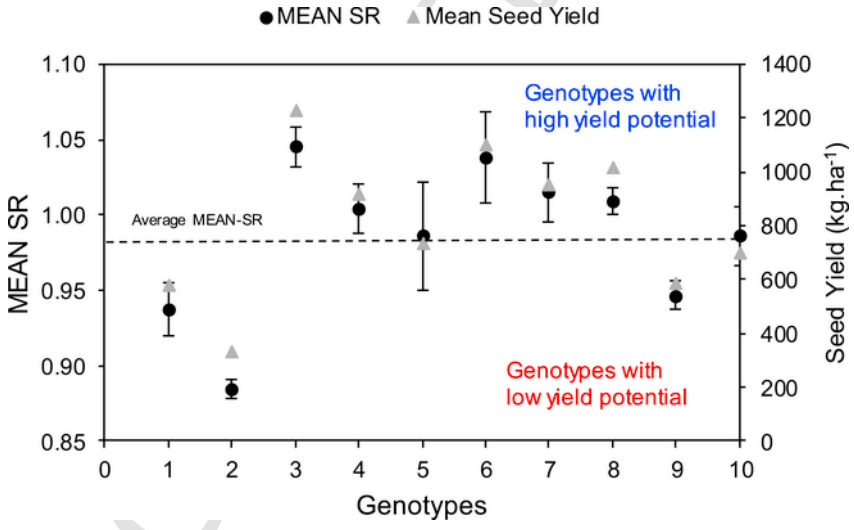

Fig. 6. Yield potential and MEAN SR data acquired from images at 72 DAP of genotypes in experiment 1503.

in part, by USDA National Institute for Food and Agriculture, Agriculture and Food Research Initiative Competitive Grant number 1011741 and the USDA-ARS CRIS project 5348-21000-024-00D.

List of abbreviations

AGL	Above ground level
DAP	Days after planting
DN	Digital numbers
G	Green
GNDVI	Green normalized difference vegetation index
MAX	Maximum value extracted from specific vegetation index data
MEAN	Mean/average value extracted from specific vegetation index data
MIN	Minimum value extracted from specific vegetation index data
NDVI	Normalized difference vegetation index
NIR	Near infrared
R_G	DN represent reflectance at green spectral band
R_{NIR}	DN represent reflectance at near infrared spectral band
R_R	DN represent reflectance at red spectral band
R	Red
SAVI	Soil adjusted vegetation index
SR	Simple ratio
SUM	Sum of all pixels extracted from specific vegetation index data
UAV	unmanned aerial vehicle

VI vegetation index

Appendix A. Supplementary data

Supplementary data to this article can be found online at https://doi.org/10.1016/j.eaef.2019.06.002.

Uncited references

Aguera et al., 2015, Moutinho et al., 2015, Pei et al., 2018.

References

Araus, J., Cairns, J., 2014. Field high-throughput phenotyping: the new crop breeding frontier. Trends Plant Sci. 19, 152–161.

Aguera, F., Carvajal, F., Perez, M., Orgaz, F., 2015. Multi-temporal imaging using an unmanned aerial vehicle for monitoring a sunflower crop. Biosyst. Eng. 132, 19–27.

Bareth, G., Bolten, A., Hollberg, J., Aasen, H., Burkart, A., Schellberg, J., 2015. Feasibility study of using non-calibrated UAV-based RGB imagery for grassland monitoring: case study at the Rengen Long-term Grassland Experiment (RGE), Germany. DGPF Tagungsband 24, 1–7.

Basnyat, P., McConkey, B., Lafond, G., Moulin, A., Pelcat, Y., 2004. Optimal time for remote sensing to relate to crop grain yield on the Canadian prairies. Can. J. Plant Sci. 97–103.

Bendig, J., Bolten, A., Bennerts, S., Broscheit, J., Eichfuss, S., Bareth, G., 2014. Estimating biomass of barley using crop surface models (CSMs) derived from UAV-based RGB imaging. Rem. Sens. 66 (11), 10395–10412.

Brandão, Z.N., Sofiatti, V., Bezerra, J.R.C., Ferreira, G.B., 2011. Estimativa da produtividade do algodoeiro através de imagens de satélite. 8º Congresso Brasileiro de Algodão & I Cotton Expo 2011, São Paulo, 1602–1609.

Bunting, P., Clewley, D., Lucas, R.M., Gillingham, S., 2014. The remote sensing and GIS software library (RSGISLib). Comput. Geosci. 62, 216–226.

Candiago, S., Remondino, F., De Giclio, M., Dubbini, M., Gattelli, M., 2015. Evaluating multispectral images and vegetation indices for precision farming applications from UAV images. Rem. Sens. 7 (4), 4053-4047.

Chen, J.M., 2018. Remote sensing of leaf area index and clumping index. Compr. Rem. Sens. 3, 53–77.

Cheng, P., Holdsworth, W., Ma, Y., Coyne, C.J., Mazourek, M., Grusak, M.A., Fuchs, S., McGee, R.J., 2015. Association mapping of agronomic and quality traits in USDA pea single-plant collection. Mol. Breed. 35, 75.

Coyne, C.J., McGee, R.J., Redden, R.J., Ambrose, M.J., Furman, B.J., Miles, C.A., 2011. Chapter 8: genetic adjustment to changing climates: pea. Crop adaptation to climate change. Crop Adap. Clim. Change 238–250.

Dhond, S., Wuyts, N., Izné, D., 2013. Cell to whole-plant phenotyping: the best is yet to come. Cell Press 18 (8), 428–439.

Duan, T., Chapman, S.C., Guo, Y., Zheng, B., 2017. Dynamic monitoring of NDVI in wheat agronomy and breeding trials using an unmanned aerial vehicle. Field Crop. Res. 210, 71–80.

Fang, H., Liang, S., Hoogenboom, G., Teasdale, J., Cavigelli, M., 2008. "Corn-yield estimation through assimilation of remotely sensed data into the CSM-CERES-Maize model. Int. J. Remote Sens. 29, 3011–3032.

Glenn, P.E., Huete, A.R., Nagler, P.L., Nelson, S.G., 2008. Relationship between remotely-sensed vegetation indices, canopy attributes and plant physiological processes: what vegetation indices can and cannot tell us about the landscape. Sensors 8 (4), 2136–2160.

Gu, Y., Wylie, B.K., Howard, D.M., Phuyal, K.P., Ji, L., 2013. NDVI saturation adjustment: a new approach for improving cropland performance estimates in the Greater Platte River Basin. USA. Ecol. Indicat. 30, 1–6.

Haghighattalab, A., Pérez, L.G., Mondal, S., Singh, D., Schinstock, D., Rutkoski, J., Ortiz-Monasterio, I., Singh, R.P., Goodin, D., Poland, J., 2016. Application of unmanned aerial systems for high throughput phenotyping of large wheat breeding nurseries. Plant Methods 12 (1), 35.

Hu, P., Chapman, S., Wang, X., et al., 2018. Estimation of plant height using a high throughput phenotyping platform based on unmanned aerial vehicle and self-calibration: example for sorghum breeding. Eur. J. Agron. 95, 24–32.

Huete, A.R., Liu, H., van Leeuwen, J.D., 1997. The Use of Vegetation Indices in Forested Regions: Issues of Linearity and Saturation. IGARSS '97. Remote Sensing - A Scientific Vision for Sustainable Development. IEEE International, 1966–1968.

Kalu, B.A., Fick, G.W., 1981. Quantifying morphological development of alfalfa for studies of herbage quality. Crop Sci. 21 (2), 267–271.

Lebourgeois, V., Bégué, A., Labbé, S., Mallavan, B., Prévot, L., Roux, B., 2008. Can commercial digital cameras be used as multispectral sensors? A crop monitoring test. Sensors 8, 7300–7322.

McGee, R.J., McPhee, K.E., 2012. Release of autumn-sown pea germplasm ps03101269 with food-quality seed characteristics. J. Plant Registrations 6, 354–357.

McGee, R.J., Nelson, H., McPhee, K.E., 2013. "Registration of 'Lynx' winter pea. J. Plant Registrations 7, 261–264.

McGee, R.J., Coyne, C.J., Pilet-Nayel, M.L., Moussart, A., Tivoli, B., Baranger, A., Hamon, C., Vandemark, G., McPhee, K., 2012. Registration of pea germplasm lines partially resistant to aphanomyces root rot for breeding fresh or freezer pea and dry pea types. J. Plant Registrations 6, 203–207.

McPhee, K.E., Muehlbauer, F.J., 2002. Registration of 'franklin' green dry pea (Registrations of cultivars). Crop Sci. 42, 1378–1379.

McPhee, K.E., Muehlbauer, F.J., 2004. Registration of 'Stirling' green dry pea. Crop Sci. 44, 1868–1870.

McPhee, K., 2003. Dry pea production and breeding: a minireview. J. Food Agric. Environ. 1, 64–69.

Mkhabela, M.S., Bullock, P., Raj, S., Wang, S., Yang, Y., 2011. Crop yield forecasting on the Canadian Prairies using MODIS NDVI data. Agric. For. Meteorol. 151 (3), 385–393.

Moutinho, , Rodrigues, A., Sousa, J.J., Gonçalves, J.A., Bento, R., 2015. Estudo comparativo de software fotogramétrico em diferentes ambientes com RPAS: comercial vs. Open Source. In: VIII Conferencia Nacional de Cartografia e Geodesia. pp. 29–30.

Muehlbauer, F.J., Temple, S.R., Chen, W., 2004. Registration of 'sierra' chickpea. Crop Sci. 44 (5), 1864–1865.

Muehlbauer, F.J., Temple, S.R., Chen, W., 2006. Registration of dylan chickpea. Crop Sci. 46, 2705.

Muehlbauer, F.J., Van Rheenen, H.A., Kaiser, W.J., 1998. "Registration of 'myles' chickpea. Crop Sci. 38, 283.

Murillo, P., Carbonel, J., 2012. Principios y aplicaciones de la precepción remota en el cultivo de la caña de azúcar en Colombia. Centro de Investigación de la Caña de Azúcar, CENICAÑA, 181.

Munier-Jolain, N., Biarnès, V., Chaillet, I., Lecoeur, J., Jeuffroy, M., 2010. Physiology of the Pea Crop. Science Publishers, 300.

Paiva, C., Tsukahara, R., França, G., 2013. Estimativa da produtividade da cultura do trigo via SR no município de Piraí do Sul, no Estado do Paraná. In: Anais XVI Simpósio Brasileiro de SR – SBSR. pp. 158–164.

Pei, F., Wu, C., Liu, X., Li, X., Yang, K., Zhou, Y., Wang, K., Xu, L., Xia, G., 2018. Monitoring the vegetation activity in China using vegetation health indices. Agric. For. Meteorol. 248, 215–227.

Pratap, A., Gupta, S., Nair, R.M., Gupta, S.K., Schafleitner, R., Basu, P.S., Singh, C.M., Prajapati, U., Gupta, A.K., Nayyar, H., Mishra, A.K., Baek, K.H., 2019. Using plant phenomics to exploit the gains of genomics. Agronomy 9, 126.

Qi, J., Chehbouni, A., Huete, A.R., Kerr, Y.H., Sorooshian, S., 1994. A modified soil adjusted vegetation index. Rem. Sens. Environ. 48, 119–126.

Quirós, J.J., Zhang, C., Smitchger, J.A., McGee, R.J., Sankaran, S., 2019. Phenotyping of plant biomass and performance traits using remote sensing techniques in pea (pisum sativum, L.). Sensors 19, 2031.

Rao, P.V.K., Rao, V.V., Venkataratnam, L., 2002. Remote sensing: a technology for assessment of sugarcane crop acreage and yield. Sugar Tech 4, 97–101.

Sankaran, S., Zhou, J., Khot, L.R., Trapp, J.J., Mndolwa, E., Miklas, P.N., 2018. High-throughput field phenotyping in dry bean using small unmanned aerial vehicle based multispectral imagery. Comput. Electron. Agric. 151, 84–92.

Sankaran, S., Khot, L.R., Espinoza, C.Z., Jarolmasjed, S., Sathuvalli, V.R., Vandemark, G.J., Miklas, P.N., Carter, A.H., Pumphrey, M.O., Knowles, N.R., Pavek, M.J., 2015. Low-altitude, high-resolution aerial imaging systems for row and field crop phenotyping: a review. Eur. J. Agron. 70, 112–123.

Saxena, M.C., Hawtin, G.C., 1981. Morphology and growth patterns. Lentils. Slough, CAB 39–52.

Serrano, L., Filella, I., Penuelas, J., 2000. Remote sensing of biomass and yield of winter wheat under different nitrogen supplies. Crop Sci. 40, 723–731.

Shanahan, J.F., Schepers, J.S., Francis, D.D., Varvel, G.E., Wilhelm, W.W., Tringe, J.M., Schlemmer, M.R., Major, D.J., 2001. Use of remote-sensing imagery to estimate corn grain yield. Agron. J. 93, 583–589.

Shi, Y., Thomasson, J.A., Murray, S.C., Pugh, N.A., Rooney, W.L., Shafian, S., Rajan, N., Rouze, G., Morgan, C.L., Neely, H.L., Rana, A., 2016. Unmanned aerial vehicles for high-throughput phenotyping and agronomic research. PLoS One 11 (7), 26.

Shirabe, T., 2011. Prescriptive modeling with map Algebra for Multi-Zone allocation with size constraints. 36 (5), 456–469.

Sid'ko, A.F., Botvich, I.Yu., Pisman, T.I., Shevyrnogov, A.P., 2017. Estimation of chlorophyll content and yield of wheat crops from reflectance spectra obtained by ground-based remote measurements. Field Crop. Res. 207, 24–29.

Swain, K.C., Thomson, S.J., Jayasuriya, H.P., 2010. Adoption of an unmanned helicopter for low-altitude remote sensing to estimate yield and total biomass of a rice crop. Trans. ASABE 53, 21–27.

Tagil, S., Jenness, J., 2008. GIS-based automated landform classification and topographic, landcover and geologic attributes of landforms around the Yazoren polje, Turkey. J. Appl. Sci. 8 (6), 910–921.

Tennakoon, S.B., Murty, V.V.N., Eiumnoh, A., 1992. Estimation of cropped area and grain yield of rice using remote sensing data. Int. J. Remote Sens. 13, 427–439.

Thenkabail, P., Lyon, J., 2012. Hyperspectral Remote Sensing of Vegetation. CRC Press, Boca Raton, 782.

Vandemark, G., Guy, S.O., Chen, W., McPhee, K., Pfaff, J., Lauver, M., Muehlbauer, F.J., 2015. Registration of 'Nash'Chickpea. J. Plant Registrations 9 (3), 275–278.

Vandemark, G., Muehlbauer, F.J., Mihov, M., Chen, W., McPhee, K., Chen, C., 2014. Registration of CA0469C025C chickpea germplasm. J. Plant Registrations 8 (3), 303–307.

Vega, F., Carvajal, F., Perez, M., Orgaz, F., 2015. Multi-temporal imaging using an unmanned aerial vehicle for monitoring a sunflower crop. Biosyst. Eng. 132, 19–27.

Wang, J., Rich, P.M., Price, K.P., 2003. Temporal responses of NDVI to precipitation and temperature in the central Great Plains, USA. Int. J. Remote Sens. 24 (11), 2345–2364.

Xiao, X., Boles, S., Frolking, S., Salas, W., Moore III, B., Li, C., 2002. Observation of flooding and rice transplanting of paddy rice fields at the site to landscape scales in China using VEGETATION sensor data. Int. J. Remote Sens. 23 (15), 3009–3022.

Yao, F., Tang, Y., Wang, P., Zhang, J., 2015. Estimation of maize yield by using a process-based model and remote sensing data in the Northeast China Plain. Phys. Chem. Earth 87, 142–152.

Yu, N., Li, L., Schmitz, N., Tian, L., Greenberg, J., Diers, B., 2016. Development of methods to improve soybean yield estimation and predict plant maturity with an unmanned aerial vehicle based platform. Rem. Sens. Environ. 187, 91–101.

Zając, T., Klimek-Kopyra, A., Oleksy, A., Stokłosa, A., Kulig, B., 2012. Morphological-developmental reaction and productivity of plants and canopy of semileafless pea (Pisum sativum L.) after seed vaccination with Rhizobium and foliar micronutrient fertilization. J. Appl. Bot. Food Qual. 85, 188–197.

Zhang, C., Kovacs, M., 2012. The application of small unmanned aerial systems for precision agriculture: a review. Precis. Agric. 13, 693–712.

Zhou, X., Zheng, H.B., Xu, X.Q., He, J.Y., Yao, X., Cheng, T., Zhu, Y., Cao, W.X., Tian, Y.C., 2017. Predicting grain yield in rice using multi-temporal vegetation indices from UAV-based multispectral and digital imagery. ISPRS J. Photogrammetry Remote Sens. 130, 246–255.